

Markovian Treatment of non-Markovian Dynamics of Open Fermionic Systems

Feng Chen,¹ Enrico Arrigoni,² and Michael Galperin^{3,*}

¹*Department of Physics, University of California San Diego, La Jolla, CA 92093, USA*

²*Institute of Theoretical and Computational Physics,
Graz University of Technology, 8010 Graz, Austria*

³*Department of Chemistry & Biochemistry, University of California San Diego, La Jolla, CA 92093, USA*

We show that an open fermionic system coupled to continuous environment with unitary system-environment evolution can be exactly mapped onto an auxiliary system consisting of the physical fermion system and a set of discrete fermionic modes subject to non-unitary Lindblad-type system-modes evolution in such a way that reduced dynamics of the fermionic system in the two cases are the same. Conditions for equivalence of reduced dynamics in the two systems are identified and a proof is presented. The study is extension of recent work on Bose systems [D. Tamascelli, A. Smirne, S. F. Huelga, and M. B. Plenio, Phys. Rev. Lett. **120**, 030402 (2018)] to open quantum Fermi systems and to multi-time correlation functions. Numerical simulations within generic junction model are presented for illustration.

I. INTRODUCTION

Open nonequilibrium systems are at the forefront of experimental and theoretical research due to rich and complex physics they provide access to as well as due to applicational prospects of building nanoscale devices for quantum based technologies and computations¹⁻³. Especially intriguing in term of both fundamental science and potential applications are effects of strong correlations. A number of impurity solvers capable of treating strongly correlated systems coupled to continuum of baths degrees of freedom were developed. Among them are numerical renormalization group in the basis of scattering states^{4,5}, flow equations^{6,7}, time-dependent density matrix renormalization group^{8,9}, multilayer multiconfiguration time-dependent Hartree (ML-MCTDH)^{10,11}, and continuous time quantum Monte Carlo¹²⁻¹⁴ approaches. These numerically exact techniques are very demanding and so far are mostly applicable to simple models only.

At the same time, accurate numerically inexpensive impurity solvers are in great demand both as standalone techniques to be applied in simulation of, e.g., nanoscale junctions and as a part of divide-and-conquer schemes such as, e.g, dynamical mean-field theory (DMFT)^{15,16}. In this respect ability to map complicated non-Markovian dynamics of a system onto much simpler Markov consideration is an important step towards creating new computational techniques applicable in realistic simulations. In particular, such mapping was used in auxiliary master equation approach (AMEA)^{17,18} introducing numerically inexpensive and pretty accurate solver for the nonequilibrium DMFT. Another example is recent formulation of the auxiliary dual-fermion method¹⁹. While the mappings appear to be very useful and accurate, only semi-quantitative arguments for possibility of the mapping were presented with main supporting evidence being benchmarking vs. numerically exact computational techniques. In particular, a justification for the mapping was argued in Refs.²⁰⁻²² based upon the singular coupling derivation of the Lindblad equation. Still, the

consideration is not rigorous.

Recently, a rigorous proof of non-Markov to Markov mapping for open Bose quantum systems was presented in the literature²³. It was shown that evolution of reduced density matrix in non-Markov system with unitary system-environment evolution can be equivalently presented by Markov evolution of an extended system (system plus modes of environment) under non-unitary (Lindblad-type) evolution. Here, we extend consideration of Ref.²³ to fermionic open quantum systems and to multi-time correlation functions. The structure of the paper is the following. After introducing physical and auxiliary models of an open quantum Fermi system in Section II we discuss non-Markov to Markov mapping procedure in Section III. Exact mathematical proofs are given in Appendices. Section IV presents numerical illustration of the mapping for a simple generic model of a junction. We conclude in Section V.

II. MODELS

We consider an open fermionic system S coupled to an arbitrary number N of external baths, initially each at its

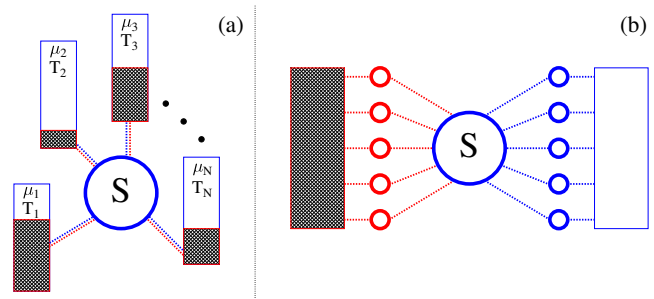


FIG. 1: Sketch of an open fermionic system S . Shown are (a) physical system coupled to N baths and (b) illustration for an auxiliary system with coupling to full (left) and empty (right) baths.

own thermodynamic equilibrium, i.e. characterized by its own electrochemical potential and temperature (see Fig. 1a). The Hamiltonian of the model is

$$\hat{H}^{phys}(t) = \hat{H}_S(t) + \sum_{B=1}^N \left(\hat{H}_B + \hat{V}_{SB} \right) \quad (1)$$

Here $\hat{H}_S(t)$ and \hat{H}_B ($K \in \{1, \dots, N\}$) are Hamiltonians of the system and baths. \hat{V}_{SB} introduces coupling of the system to bath B . While the Hamiltonian of the system is general and may be time-dependent, we follow the usual paradigm by assuming bi-linear coupling in constructing fermionic junction models.

$$\hat{H}_B = \sum_{k \in B} \varepsilon_{Bk} \hat{c}_{Bk}^\dagger \hat{c}_{Bk} \quad (2)$$

$$\hat{V}_{SB} = \sum_{k \in B} \sum_{i \in S} \left(V_{i,Bk} \hat{d}_i^\dagger \hat{c}_{Bk} + H.c. \right) \quad (3)$$

where \hat{d}_i^\dagger (\hat{d}_i) and \hat{c}_{Bk}^\dagger (\hat{c}_{Bk}) create (annihilate) electron in level i of the system S and level k of bath B . In the model, dynamics of the system-plus-baths evolution is unitary. Below we call this model *phys* (physical). We note in passing that extension of the consideration to other types of system-baths couplings is straightforward, as long as baths are quadratic in the Fermi operators.

The other configuration we'll consider is a model we shall call *aux* (auxiliary; see Fig. 1b). Here, the same system S is coupled to a number of auxiliary modes A , which in their turn are coupled to two baths. There are two Fermi baths in the configuration: one (L) is completely full ($\mu_L \rightarrow +\infty$), the other (R) is completely empty ($\mu_R \rightarrow -\infty$). The Hamiltonian of the system is

$$\hat{H}^{aux}(t) = \hat{H}_S(t) + \hat{V}_{SA} + \hat{H}_A + \sum_{C=L,R} \left(\hat{H}_C + \hat{V}_{AC} \right) \quad (4)$$

where \hat{H}_S is the same as in (1), \hat{H}_A represents set of modes

$$\hat{H}_A = \sum_{m_1, m_2 \in A} H_{m_1 m_2}^A \hat{a}_{m_1}^\dagger \hat{a}_{m_2} \quad (5)$$

and \hat{V}_{SA} their interaction with the system

$$\hat{V}_{SA} = \sum_{i \in S} \sum_{m \in A} \left(V_{im}^{SA} \hat{d}_i^\dagger \hat{a}_m + H.c. \right) \quad (6)$$

Here \hat{a}_m^\dagger (\hat{a}_m) creates (annihilates) electron in the auxiliary mode m in A .

\hat{H}_C represents continuum of states in contact C

$$\hat{H}_C = \sum_{k \in C} \varepsilon_{Ck} \hat{c}_{Ck}^\dagger \hat{c}_{Ck} \quad (7)$$

with constant density of states

$$N_C(E) \equiv \sum_{k \in C} \delta(E - \varepsilon_{Ck}) = const \quad (8)$$

and \hat{V}_{AC} couples auxiliary modes A to bath C (L or R)

$$\hat{V}_{AC} = \sum_{k \in C} \sum_{m \in A} \left(t_m^C \hat{a}_m^\dagger \hat{c}_{Ck} + H.c. \right) \quad (9)$$

Dynamics of the whole configuration is unitary.

In the next section we show that the reduced time evolution of S in models *phys* and *aux* is the same (subject to certain conditions) and that the reduced dynamics of $S + A$ in model *aux* satisfies an appropriate Lindblad Markov evolution. This establishes procedure for Markov non-unitary Lindblad-type treatment of $S + A$ in *aux* exactly representing unitary non-Markov dynamics of S in *phys* by tracing out A degrees of freedom.

III. NON-MARKOV TO MARKOV MAPPING

First, we are going to prove that with an appropriate choice of parameters of *aux* the dynamics of S can be equivalently represented in the original model *phys* and auxiliary model *aux*, under assumption that the dynamics of the whole system is unitary. Because non-interacting baths are fully characterized by their two-time correlation functions, equivalence of system-bath(s) hybridizations (i.e. correlation functions of the bath(s) dressed with system-bath(s) interactions) for the two models indicates equivalence of the reduced system dynamics in the two cases. For example, hybridization function is the only information about baths in numerically exact simulations of strongly correlated systems¹³. Nonequilibrium character of the system requires fitting two projections of the hybridization function (also called self-energy in the literature). In particular, these may be retarded and Keldysh projections. Let $\Sigma_B^r(E)$ and $\Sigma_B^K(E)$ are matrices introducing the corresponding hybridization functions for bath α of the physical problem (Fig. 1a).

$$\left(\Sigma_B^r(E) \right)_{ij} = \sum_{k \in B} V_{i,Bk} g_{Bk}^r(E) V_{Bk,j} \quad (10)$$

$$\left(\Sigma_B^K(E) \right)_{ij} = \sum_{k \in B} V_{i,Bk} g_{Bk}^K(E) V_{Bk,j} \quad (11)$$

where $g_{Bk}^{r(K)}(E)$ are the Fourier transforms of retarded (Keldysh) projections of the free electron Green's function $g_{Bk}(\tau, \tau') = -i \langle T_c \hat{c}_{Bk}(\tau) \hat{c}_{Bk}^\dagger(\tau') \rangle$. Then total hybridization functions for the system

$$\Sigma^r(E) = \sum_{B=1}^N \Sigma_B^r(E) \quad (12)$$

$$\Sigma^K(E) = 2i \sum_{B=1}^N \left(1 - 2f_B(E) \right) \text{Im} \Sigma_B^r(E) \quad (13)$$

should be identical with the corresponding hybridization functions, $\tilde{\Sigma}^r(E)$ and $\tilde{\Sigma}^K(E)$, of S in the auxiliary model (Fig. 1b). The latter have contribution from full (L) and empty (R) baths, and from auxiliary modes (A)

$$\tilde{\Sigma}^r(E) = \tilde{\Sigma}_L^r(E) + \tilde{\Sigma}_R^r(E) \quad (14)$$

$$\tilde{\Sigma}^K(E) = 2i \text{Im} \left(\tilde{\Sigma}_R^r(E) - \tilde{\Sigma}_L^r(E) \right) \quad (15)$$

where we assume modes A initially in stationary state. Requirement of equivalence can be expressed as

$$\text{Im } \tilde{\Sigma}_L^r(E) = \frac{2i \text{Im} \Sigma^r(E) + \Sigma^K(E)}{4i} \quad (16)$$

$$\text{Im } \tilde{\Sigma}_R^r(E) = \frac{2i \text{Im} \Sigma^r(E) - \Sigma^K(E)}{4i} \quad (17)$$

Thus, the problem reduces to fitting known functions in the right side of the expression with multiple contributions from auxiliary modes to the hybridization functions in the left side. In principle, this fitting can be done in many different ways²¹. For example, possibility of exact fitting of an arbitrary function with set of Lorentzians was discussed in Ref.²⁴. In auxiliary systems such fitting corresponds to a construction where each auxiliary mode is coupled to its own bath. Note that in practical simulations accuracy of the results can be improved either by increasing number of auxiliary modes, as is implemented in, e.g, AMEA²⁵, or by employing diagrammatic expansion related to the difference between true and fitted hybridization functions, as is realized in, e.g., dual fermion approach²⁶, or both.

Now, when equivalence of reduced system (S) dynamics in *phys* and *aux* is established, we turn to consideration of evolution of the *aux* model. We will show that reduced $S+A$ dynamics derived from unitary evolution of the *aux* model can be exactly represented by non-unitary Lindblad-type evolution.

Following Ref.²³ we consider reduced density operator of $S+A$ in *aux*, $\hat{\rho}_{SA}$, which is defined by integrating out baths degrees of freedom of the total density operator $\hat{\rho}^{aux}(t)$

$$\hat{\rho}_{SA}(t) \equiv \text{Tr}_{LR} \left[\hat{\rho}^{aux}(t) \right] \quad (18)$$

The latter follows unitary evolution with initial condition being $S+A$ decoupled from the baths

$$\hat{\rho}^{aux}(0) = \hat{\rho}_L \otimes \hat{\rho}_{SA}(0) \otimes \hat{\rho}_R \quad (19)$$

where $\hat{\rho}_L = |full\rangle\langle full|$ and $\hat{\rho}_R = |empty\rangle\langle empty|$.

In Appendix A we prove that $\hat{\rho}_{SA}(t)$ satisfies Markov Lindblad-type equation of motion

$$\begin{aligned} \frac{d}{dt} \hat{\rho}_{SA}(t) &= -i \left[\hat{H}_{SA}(t), \hat{\rho}_{SA}(t) \right] + \sum_{m_1, m_2 \in A} \left[\right. \\ &\Gamma_{m_1 m_2}^R \left(\hat{a}_{m_2} \hat{\rho}_{SA}(t) \hat{a}_{m_1}^\dagger - \frac{1}{2} \{ \hat{\rho}_{SA}(t), \hat{a}_{m_1}^\dagger \hat{a}_{m_2} \} \right) \\ &+ \Gamma_{m_1 m_2}^L \left(\hat{a}_{m_1}^\dagger \hat{\rho}_{SA}(t) \hat{a}_{m_2} - \frac{1}{2} \{ \hat{\rho}_{SA}(t), \hat{a}_{m_2} \hat{a}_{m_1}^\dagger \} \right) \left. \right] \\ &\equiv \mathcal{L}_{SA}(t) | \rho_{SA}(t) \rangle \rangle \end{aligned} \quad (20)$$

where

$$\hat{H}_{SA}(t) \equiv \hat{H}_S(t) + \hat{V}_{SA} + \hat{H}_A, \quad (21)$$

\mathcal{L}_{SA} is the Liouvillian superoperator defined on the $S+A$ subspace of the *aux* model and

$$\Gamma_{m_1 m_2}^C \equiv 2\pi t_{m_1}^C (t_{m_2}^C)^* N_C \quad (C = L, R) \quad (22)$$

- (forward branch)



+ (backward branch)

FIG. 2: The Keldysh contour.

is the dissipation matrix due to coupling to contact C .

Next we turn to multi-time correlation functions of operators in the $S+A$ subspace of the *aux* model. Following Ref.²³ we start consideration from two-time correlation function on real time axis. For arbitrary operators \hat{O}_1 and \hat{O}_2 in $S+A$ we define two-time ($t_1 \geq t_2 \geq 0$) correlation function as

$$\begin{aligned} \langle \hat{O}_1(t_1) \hat{O}_2(t_2) \rangle &\equiv \quad (23) \\ \text{Tr} \left[\hat{O}_1 \hat{U}^{aux}(t_1, t_2) \hat{O}_2 \hat{U}^{aux}(t_2, 0) \hat{\rho}^{aux}(0) \hat{U}^{aux\dagger}(t_1, 0) \right] \end{aligned}$$

Here \hat{U}^{aux} is the evolution operator in the *aux* system

$$\hat{U}^{aux}(t, t') \equiv T \exp \left[-i \int_{t'}^t ds \hat{H}^{aux}(s) \right] \quad (24)$$

and T is the time-ordering operator. In B we show that (23) can be equivalently obtained from reduced Lindblad-type evolution in the $S+A$ subspace

$$\begin{aligned} \langle \hat{O}_1(t_1) \hat{O}_2(t_2) \rangle &= \quad (25) \\ \langle \langle I | \mathcal{O}_1^- \mathcal{U}_{SA}(t_1, t_2) \mathcal{O}_2^- \mathcal{U}_{SA}(t_2, 0) | \rho_{SA}(0) \rangle \rangle \end{aligned}$$

Here $\langle \langle I |$ is Liouville space bra representation of the Hilbert space identity operator, \mathcal{O}_i is the Liouville space superoperator corresponding to the Hilbert space operator \hat{O}_i (see Fig. 2)

$$\mathcal{O}_i | \rho \rangle \rangle = \begin{cases} \mathcal{O}_i^- | \rho \rangle \rangle \equiv \hat{O}_i \hat{\rho} & \text{forward branch} \\ \mathcal{O}_i^+ | \rho \rangle \rangle \equiv \hat{\rho} \hat{O}_i & \text{backward branch} \end{cases} \quad (26)$$

and \mathcal{U}_{SA} is the Liouville space evolution superoperator

$$\mathcal{U}_{SA}(t, t') \equiv T \exp \left[\int_{t'}^t ds \mathcal{L}_{SA}(s) \right] \quad (27)$$

Finally, we extend consideration to multi-time correlation functions of arbitrary operators \hat{O}_i ($i \in \{1, \dots, N\}$) defined on the Keldysh contour (see Fig. 2) as

$$\begin{aligned} \langle T_c \hat{O}_1(\tau_1) \hat{O}_2(\tau_2) \dots \hat{O}_N(\tau_N) \rangle &\equiv \quad (28) \\ \text{Tr} \left[T_c \hat{O}_1 \hat{O}_2 \dots \hat{O}_N \hat{U}_c \hat{\rho}^{aux}(0) \right] \end{aligned}$$

where τ_i are the contour variables, T_c is the contour ordering operator, and

$$\hat{U}_c = T_c \exp \left[-i \int_c d\tau \hat{H}^{aux}(\tau) \right] \quad (29)$$

is the contour evolution operator. Note subscripts of operators O_i in the right side of (28) indicate both type of the operator and its position on the contour. In C we prove that multi-time correlation functions (28) can be evaluated solely from Markov Lindblad-type evolution in $S + A$ subspace of the aux model

$$\begin{aligned} \langle T_c \hat{O}_1(\tau_1) \hat{O}_2(\tau_2) \dots \hat{O}_N(\tau_N) \rangle = & \quad (30) \\ (-1)^P \langle \langle I | \mathcal{O}_{\theta_1} \mathcal{U}_{SA}(t_{\theta_1}, t_{\theta_2}) \mathcal{O}_{\theta_2} \mathcal{U}_{SA}(t_{\theta_2}, t_{\theta_3}) \dots & \\ \dots \mathcal{O}_{\theta_N} \mathcal{U}_{SA}(t_{\theta_N}, 0) | \rho_{SA}(0) \rangle \rangle & \end{aligned}$$

Here P is number of Fermi interchanges in the permutation of operators \hat{O}_i by T_c , θ_i are indices of operators \hat{O}_i rearranged in such a way that $t_{\theta_1} > t_{\theta_2} > \dots > t_{\theta_N}$ (t_{θ_i} is real time corresponding to contour variable τ_{θ_i}), \mathcal{O}_{θ_i} are the superoperators defined in (26), and \mathcal{U}_{SA} is the Liouville space evolution superoperator defined in (27).

Equivalence of S dynamics derived from unitary evolution of models *phys* and *aux* together with (20) and (30) completes proof of possibility of Markov treatment for non-Markovian dynamics in open quantum Fermi systems.

IV. NUMERICAL ILLUSTRATION

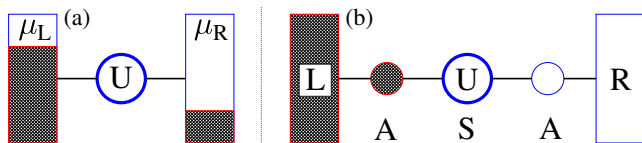


FIG. 3: Original Anderson impurity (a) and corresponding auxiliary (b) models.

Here we present numerical simulation illustrating equivalence of original unitary and Lindblad-type Markov treatment for the open quantum Fermi system. We consider Anderson model (Fig. 3a)

$$\begin{aligned} \hat{H} = & \sum_{\sigma \in \{\uparrow, \downarrow\}} \varepsilon_0 \hat{d}_\sigma^\dagger \hat{d}_\sigma + U \hat{n}_\uparrow \hat{n}_\downarrow & (31) \\ + & \sum_{k \in L, R} \sum_{\sigma \in \{\uparrow, \downarrow\}} \left(\varepsilon_k \hat{c}_{k\sigma}^\dagger \hat{c}_{k\sigma} + V_k \hat{d}_\sigma^\dagger \hat{c}_{k\sigma} + V_k^* \hat{c}_{k\sigma}^\dagger \hat{d}_\sigma \right) \end{aligned}$$

where $\hat{n}_\sigma = \hat{d}_\sigma^\dagger \hat{d}_\sigma$. We calculate the system evolution after connecting initially empty site to baths at time $t = 0$. Parameters of the simulations are (numbers are in arbitrary units of energy E_0): $\varepsilon_0 = 0$ and $U = 1$. We assume

$$\Gamma_K(E) = \gamma_K \frac{t_K^2}{(E - \varepsilon_0)^2 + (\gamma_K/2)^2} \quad (32)$$

where $\Gamma_K(E) \equiv 2\pi \sum_{k \in K} |V_k|^2 \delta(E - \varepsilon_k)$ is the electron escape rate into contact K , $\gamma_L = \gamma_R = 0.2$, and $t_L = t_R = 1$.

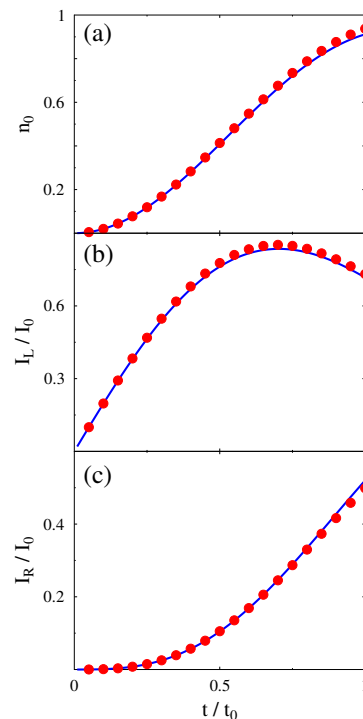


FIG. 4: Unitary (filled circles, red) and Lindblad-type (solid line, blue) evolution in auxiliary model of Fig. 3b after connecting initially empty central site to filled L and empty R baths. Shown are population of the level (a) and left (b) and right (c) currents. See text for parameters.

For simplicity, we consider high bias, so that auxiliary model with only two sites (Fig. 3b) is sufficient to reproduce dynamics in the physical system. In the auxiliary model we compare unitary evolution calculated within numerically exact td-DMRG^{8,9,27,28} with Lindblad QME results. Time is shown in units of $t_0 = \hbar/E_0$, currents use $I_0 = E_0/\hbar$, and \hbar is assumed to be 1. Figure 4 shows level population, $n_0 = \langle \hat{n}_\sigma \rangle$, as well as left, I_L , and right, I_R , currents in the system after quench. Close correspondence between the two numerical results is an illustration for exact analytical derivations presented in Section III.

V. CONCLUSIONS

We consider open quantum Fermi system S coupled to a number of external Fermi baths each at its own equilibrium (each bath has its own electrochemical potential μ_i and temperature T_i). Evolution of the model (system plus baths) is unitary. We show that reduced dynamics of the system S in the original unitary non-Markov model can be exactly reproduced by Markov non-unitary Lindblad-type evolution of an auxiliary system, which consists of the system S coupled to a number of auxiliary modes A which in turn are coupled to two Fermi baths L and R : one full ($\mu_L \rightarrow +\infty$) and one empty ($\mu_R \rightarrow -\infty$). The proof is performed in two steps: first

we show that reduced S dynamics in the physical model is equivalent to reduced dynamics of S in the auxiliary model, when A degrees of freedom and the two baths are traced out; second, we show that reduced dynamics of $S+A$ in the auxiliary model with unitary evolution of the model can be exactly reproduced by the Lindblad-type Markov evolution of $S+A$. The correspondence is shown to hold for reduced density matrix and for multi-time correlation functions defined on the Keldysh contour. Our study is extension of recent work about Bose systems²³ to open Fermi systems and beyond only reduced density matrix consideration. Establishing possibility of exact mapping of reduced unitary non-Markov dynamics to much simpler non-unitary Markov Lindblad-type treatment sets firm basis for auxiliary quantum master equations (QME) methods employed in, e.g, AMEA¹⁷ or aux-DF¹⁹ approaches. We note that in practical implementations improving quality of mapping can be based on increasing number of A modes, as is done in advanced AMEA implementations²⁵, or by utilization of expansion in discrepancy between physical and auxiliary hybridization functions, as is done in the dual fermion formulation²⁶, or both. Scaling performance of the two approaches to mapping quality enhancement is a goal for future research.

Acknowledgments

We thank Max Sorantin for useful discussions. This material is based upon work supported by the National

Science Foundation under grant CHE-1565939.

Appendix A: Derivation of Eq. (20)

Here we prove that reduced density matrix of $S+A$ in the aux model satisfies Markov Lindblad-type equation-of-motion (EOM), Eq. (20).

We start by considering unitary evolution of the aux model. Heisenberg EOM for bath annihilation operator \hat{c}_{Ck} is

$$\begin{aligned} \frac{d}{dt}\hat{c}_{Ck}(t) &= i[\hat{H}^{aux}(t), \hat{c}_{Ck}(t)] \\ &= -i\varepsilon_{Ck}\hat{c}_{Ck}(t) - i\sum_{m\in A}(t_m^C)^*\hat{a}_m(t) \end{aligned} \quad (\text{A1})$$

Its formal solution is

$$\hat{c}_{Ck}(t) = e^{-i\varepsilon_{Ck}t}\hat{c}_{Ck}(0) - i\sum_{m\in A}(t_m^C)^*\int_0^t ds e^{i\varepsilon_{Ck}(t-s)}\hat{a}_m(s) \quad (\text{A2})$$

Thus, Heisenberg EOM for an arbitrary operator \hat{O} on $S+A$ can be written as

$$\begin{aligned} \frac{d}{dt}\hat{O}(t) &= i[\hat{H}_{SA}(t), \hat{O}(t)] - i\sum_{m\in A}\left\{ \right. \\ &\sum_{k\in R}\left[t_m^R[\hat{O}(t), \hat{a}_m^\dagger]_\zeta \left(e^{-i\varepsilon_{Rk}t}\hat{c}_{Rk}(0) - i\sum_{m'\in A}(t_{m'}^R)^*\int_0^t ds e^{-i\varepsilon_{Rk}(t-s)}\hat{a}_{m'}(s) \right) \right. \\ &\quad \left. + \zeta(t_m^R)^* \left(e^{i\varepsilon_{Rk}t}\hat{c}_{Rk}^\dagger(0) + i\sum_{m'\in A}t_{m'}^R\int_0^t ds e^{i\varepsilon_{Rk}(t-s)}\hat{a}_{m'}^\dagger(s) \right) [\hat{O}(t), \hat{a}_m(t)]_\zeta \right] \\ &- \sum_{k\in L}\left[(t_m^L)^*[\hat{O}(t), \hat{a}_m(t)]_\zeta \left(e^{i\varepsilon_{Lk}t}\hat{c}_{Lk}^\dagger(0) + i\sum_{m'\in A}t_{m'}^L\int_0^t ds e^{i\varepsilon_{Lk}(t-s)}\hat{a}_{m'}^\dagger(s) \right) \right. \\ &\quad \left. + \zeta t_m^L \left(e^{-i\varepsilon_{Lk}t}\hat{c}_{Lk}(0) - i\sum_{m'\in A}(t_{m'}^L)^*\int_0^t ds e^{-i\varepsilon_{Lk}(t-s)}\hat{a}_{m'}(s) \right) [\hat{O}(t), \hat{a}_m^\dagger(t)]_\zeta \right] \left. \right\} \end{aligned} \quad (\text{A3})$$

where $\zeta = +/- 1$ if \hat{O} contains even/odd number of fermion operators, and $[\cdot, \cdot]_\zeta$ is (anti)commutator for $\zeta = (-)1$.

For future reference we introduce

$$\hat{c}_C^{(in)}(t) \equiv \sum_{k\in C} e^{-i\varepsilon_{Ck}t}\hat{c}_{Ck}(0) \quad (\text{A4})$$

which satisfies usual commutation relations

$$\{\hat{c}_{C_1}^{(in)}(t), \hat{c}_{C_2}^{(in)\dagger}(s)\} = \delta_{C_1, C_2} \delta(t-s) \quad (\text{A5})$$

$$\{\hat{c}_{C_1}^{(in)}(t), \hat{c}_{C_2}^{(in)}(s)\} = \{\hat{c}_{C_1}^{(in)\dagger}(t), \hat{c}_{C_2}^{(in)\dagger}(s)\} = 0 \quad (\text{A6})$$

Note that because contact density of states N_C is con-

stant

holds for arbitrary function $f(t)$.

$$\sum_{k \in C} e^{-i\varepsilon_C k t} \equiv \int d\varepsilon N_C(\varepsilon) e^{-i\varepsilon t} = 2\pi N_C \delta(t) \quad (\text{A7})$$

is satisfied. Note also that

$$\int_0^t ds \delta(t-s) f(s) = \frac{1}{2} f(t) \quad (\text{A8}) \quad \text{Using (A4), (A7), and (A8) in (A3) leads to}$$

$$\begin{aligned} \frac{d}{dt} \hat{O}(t) &= i[\hat{H}_{SA}(t), \hat{O}(t)] \\ &- i \sum_{m \in A} \left\{ t_{Rj} [\hat{O}(t), \hat{a}_m^\dagger(t)]_\zeta \hat{c}_R^{(in)}(t) + \zeta (t_m^R)^* \hat{c}_R^{(in)\dagger}(t) [\hat{O}(t), \hat{a}_m(t)]_\zeta \right. \\ &\quad \left. - (t_m^L)^* [\hat{O}(t), \hat{a}_m(t)]_\zeta \hat{c}_L^{(in)\dagger}(t) - \zeta t_m^L \hat{c}_L^{(in)}(t) [\hat{O}(t), \hat{a}_m^\dagger(t)]_\zeta \right\} \\ &- \frac{1}{2} \sum_{m_1, m_2 \in A} \left\{ \Gamma_{m_1 m_2}^R [\hat{O}(t), \hat{a}_{m_1}^\dagger(t)]_\zeta \hat{a}_{m_2}(t) - \zeta \Gamma_{m_2 m_1}^R \hat{a}_{m_2}(t)^\dagger [\hat{O}(t), \hat{a}_{m_1}(t)]_\zeta \right. \\ &\quad \left. - \zeta \Gamma_{m_1 m_2}^L \hat{a}_{m_2}(t) [\hat{O}(t), \hat{a}_{m_1}^\dagger(t)]_\zeta + \Gamma_{m_2 m_1}^L [\hat{O}(t), \hat{a}_{m_1}(t)]_\zeta \hat{a}_{m_2}^\dagger(t) \right\} \end{aligned} \quad (\text{A9})$$

where we employed definition of the dissipation matrix, Eq. (22).

Next we are going to write EOM for expectation value of \hat{O}

$$\langle \hat{O}(t) \rangle \equiv \text{Tr}[\hat{O}(t) \hat{\rho}^{aux}(0)] \quad (\text{A10})$$

by averaging (A9) with initial density operator of the *aux* model, Eq. (19). Because initially $S + A$ is from the baths and because bath L is full and R is empty (see Fig. 1b)

$$\hat{c}_L^{(in)\dagger}(t) \hat{\rho}_L = \hat{\rho}_L \hat{c}_L^{(in)}(t) = \hat{c}_R^{(in)}(t) \hat{\rho}_R = \hat{\rho}_R \hat{c}_R^{(in)\dagger}(t) = 0 \quad (\text{A11})$$

holds. Thus, second and third lines in (A9) do not contribute, and EOM for the expectation value of $\hat{O}(t)$ is

$$\begin{aligned} \left\langle \frac{d}{dt} \hat{O}(t) \right\rangle &= \text{Tr} \left[\hat{\rho}^{aux}(0) i[\hat{H}_{SA}(t), \hat{O}(t)] \right] - \frac{1}{2} \sum_{m_1, m_2 \in A} \text{Tr} \left[\hat{\rho}^{aux}(0) \left\{ \right. \right. \\ &\quad \Gamma_{m_1 m_2}^R [\hat{O}(t), \hat{a}_{m_1}^\dagger(t)]_\zeta \hat{a}_{m_2}(t) - \zeta \Gamma_{m_1 m_2}^R \hat{a}_{m_1}^\dagger(t) [\hat{O}(t), \hat{a}_{m_2}(t)]_\zeta \\ &\quad \left. \left. + \Gamma_{m_1 m_2}^L [\hat{O}(t), \hat{a}_{m_2}(t)]_\zeta \hat{a}_{m_1}^\dagger(t) - \zeta \Gamma_{m_1 m_2}^L \hat{a}_{m_2}(t) [\hat{O}(t), \hat{a}_{m_1}^\dagger(t)]_\zeta \right\} \right] \end{aligned} \quad (\text{A12})$$

Because \hat{O} is arbitrary in $S + A$, after transforming to Schrödinger picture (A12) can be rewritten as EOM for $\hat{\rho}^{aux}(t)$

$$\begin{aligned} \frac{d}{dt} \hat{\rho}^{aux}(t) &= -i[\hat{H}_{SA}(t), \hat{\rho}^{aux}(t)] \\ &+ \sum_{m_1, m_2 \in A} \left[\Gamma_{m_1 m_2}^R \left(\hat{a}_{m_2} \hat{\rho}^{aux}(t) \hat{a}_{m_1}^\dagger - \frac{1}{2} \{ \hat{\rho}^{aux}(t), \hat{a}_{m_1}^\dagger \hat{a}_{m_2} \} \right) \right. \\ &\quad \left. + \Gamma_{m_1 m_2}^L \left(\hat{a}_{m_1}^\dagger \hat{\rho}^{aux}(t) \hat{a}_{m_2} - \frac{1}{2} \{ \hat{\rho}^{aux}(t), \hat{a}_{m_2} \hat{a}_{m_1}^\dagger \} \right) \right] \end{aligned} \quad (\text{A13})$$

Finally, because only operators in $S + A$ subspace appear in the right side of (A13), tracing out baths degrees of freedom leads to Eq. (20).

Appendix B: Derivation of Eq. (25)

Here we prove that two-time correlation function of two arbitrary operators in $S + A$, $\langle \hat{O}_1(t_1) \hat{O}_2(t_2) \rangle$ ($t_1 \geq t_2 \geq$

0), Eq. (23), can be equivalently obtained from reduced

Lindblad-type evolution in the $S + A$ subspace of the aux model.

Let introduce $t \equiv t_1 - t_2 \geq 0$, then $\hat{O}_1(t_1)\hat{O}_2(t_2) =$

$\hat{O}_1(t + t_2)\hat{O}_2(t_2)$ and using Eq. (A9) we get

$$\begin{aligned} \frac{d}{dt}\hat{O}_1(t + t_2)\hat{O}_2(t_2) &= \left\{ i[\hat{H}_{SA}(t + t_2), \hat{O}_1(t + t_2)] \right. \\ &- i \sum_{m \in A} \left(t_m^R [\hat{O}_1(t + t_2), \hat{a}_m^\dagger(t + t_2)]_{\zeta_1} \hat{c}_R^{(in)}(t + t_2) + \zeta_1 (t_m^R)^* \hat{c}_R^{(in)\dagger}(t + t_2) [\hat{O}_1(t + t_2), \hat{a}_m(t + t_2)]_{\zeta_1} \right. \\ &\quad \left. - (t_m^L)^* [\hat{O}_1(t + t_2), \hat{a}_m(t + t_2)]_{\zeta_1} \hat{c}_L^{(in)\dagger}(t + t_2) - \zeta_1 t_m^L \hat{c}_L^{(in)}(t + t_2) [\hat{O}_1(t + t_2), \hat{a}_m^\dagger(t + t_2)]_{\zeta_1} \right) \\ &- \frac{1}{2} \sum_{m_1, m_2 \in A} \left(\Gamma_{m_1 m_2}^R [\hat{O}_1(t + t_2), \hat{a}_{m_1}^\dagger(t + t_2)]_{\zeta_1} \hat{a}_{m_2}(t + t_2) - \zeta_1 \Gamma_{m_1 m_2}^R \hat{a}_{m_1}^\dagger(t + t_2) [\hat{O}_1(t + t_2), \hat{a}_{m_2}(t + t_2)]_{\zeta_1} \right. \\ &\quad \left. + \Gamma_{m_1 m_2}^L [\hat{O}_1(t + t_2), \hat{a}_{m_2}(t + t_2)]_{\zeta_1} \hat{a}_{m_1}^\dagger(t + t_2) - \zeta_1 \Gamma_{m_1 m_2}^L \hat{a}_{m_2}(t + t_2) [\hat{O}_1(t + t_2), \hat{a}_{m_1}^\dagger(t + t_2)]_{\zeta_1} \right) \Big\} \hat{O}_2(t_2) \end{aligned} \quad (B1)$$

Note that for $t > 0$

$$[\hat{c}_C^{(in)\dagger}(t + t_2), \hat{O}_2(t_2)]_{\zeta_2} = [\hat{c}_C^{(in)}(t + t_2), \hat{O}_2(t_2)]_{\zeta_2} = 0 \quad (B2)$$

Indeed, because from Eq. (A9) it is clear that $\hat{O}_2(t_2)$ depends on $\hat{O}_2(s)$ and $\hat{c}_C^{(in)\dagger}(s)$ only at earlier times ($s < t_2$) and because Eq. (A5) shows that $\hat{c}_C^{(in)\dagger}(s)$ taken at different times anti-commute with each other,

Eq. (B2) holds.

Thus, while taking the expectation value of (B1) with respect to $\hat{\rho}^{aux}(0)$, Eq. (19), $\hat{c}_L^{(in)\dagger}(t + t_2)$ and $\hat{c}_R^{(in)}(t + t_2)$ can be moved over $\hat{O}_2(t_2)$ for any $t > 0$. So as in A, terms with $\hat{c}_C^{(in)\dagger}(t)$ in (B1) again don't contribute (see Eq. (A11)), and we get for $t > 0$

$$\begin{aligned} \frac{d}{dt} \left\langle \hat{O}_1(t + t_2) \hat{O}_2(t_2) \right\rangle &= \text{Tr} \left[\left\{ i[\hat{H}_{SA}(t + t_2), \hat{O}_1(t + t_2)] - \frac{1}{2} \sum_{m_1, m_2 \in A} \left(\right. \right. \right. \\ &\Gamma_{m_1 m_2}^R [\hat{O}_1(t + t_2), \hat{a}_{m_1}^\dagger(t + t_2)]_{\zeta_1} \hat{a}_{m_2}(t + t_2) - \zeta_1 \Gamma_{m_1 m_2}^R \hat{a}_{m_1}^\dagger(t + t_2) [\hat{O}_1(t + t_2), \hat{a}_{m_2}(t + t_2)]_{\zeta_1} \\ &\left. \left. \left. + \Gamma_{m_1 m_2}^L [\hat{O}_1(t + t_2), \hat{a}_{m_2}(t + t_2)]_{\zeta_1} \hat{a}_{m_1}^\dagger(t + t_2) - \zeta_1 \Gamma_{m_1 m_2}^L \hat{a}_{m_2}(t + t_2) [\hat{O}_1(t + t_2), \hat{a}_{m_1}^\dagger(t + t_2)]_{\zeta_1} \right) \right\} \times \hat{O}_2(t_2) \hat{\rho}^{aux}(0) \right] \end{aligned} \quad (B3)$$

Rearranging evolution operators, Eq. (24), and separating traces over $S + A$ and $L + R$ yields

$$\left\langle \hat{O}_1(t + t_2) \hat{O}_2(t_2) \right\rangle = \text{Tr}_{SA} \left\{ \hat{O}_1 \text{Tr}_{LR} \left[\hat{U}^{aux}(t + t_2, 0) \hat{O}_2(t_2) \hat{\rho}^{aux}(0) \hat{U}^{aux\dagger}(t + t_2) \right] \right\} \quad (B4)$$

$$\frac{d}{dt} \left\langle \hat{O}_1(t + t_2) \hat{O}_2(t_2) \right\rangle = \text{Tr}_{SA} \left\{ \hat{O}_1 \frac{d}{dt} \text{Tr}_{LR} \left[\hat{U}^{aux}(t + t_2, 0) \hat{O}_2(t_2) \hat{\rho}^{aux}(0) \hat{U}^{aux\dagger}(t + t_2) \right] \right\} \quad (B5)$$

So that (B3) can be rewritten as

$$\begin{aligned} \text{Tr}_{SA} \left\{ \hat{O}_1 \frac{d}{dt} \text{Tr}_{LR} [\dots] \right\} &= \text{Tr}_{SA} \left\{ \left(\mathcal{L}_{SA}^\dagger(t) \hat{O}_1 \right) \text{Tr}_{LR} [\dots] \right\} \\ &\equiv \text{Tr}_{SA} \left\{ \hat{O}_1 \mathcal{L}_{SA}(t) \text{Tr}_{LR} [\dots] \right\} \end{aligned} \quad (B6)$$

where $\mathcal{L}_{SA}^\dagger(t)$ is adjoint²⁹ of the Liouvillian $\mathcal{L}_{SA}(t)$ de-

defined in (20), and where $\text{Tr}_{LR}[\dots]$ is used as a shorthand notation for the full expression in (B4)-(B5).

Taking into account that \hat{O}_1 is an arbitrary operator, we get

$$\frac{d}{dt} \text{Tr}_{LR} [\dots] = \mathcal{L}_{SA} \text{Tr}_{LR} [\dots] \quad (B7)$$

which has solution

$$\text{Tr}_{LR}[\dots](t) = \mathcal{U}_{SA}(t, 0) \text{Tr}_{LR}[\dots](0) \equiv \mathcal{U}_{SA}(t, 0) \hat{\mathcal{O}}_2 \hat{\rho}_{SA}(t_2) \quad (\text{B8})$$

Substituting (B8) into (B4) leads to

$$\left\langle \hat{\mathcal{O}}_1(t+t_2) \hat{\mathcal{O}}_2(t_2) \right\rangle = \text{Tr}_{LR} \left[\hat{\mathcal{O}}_1 \mathcal{U}_{SA}(t_1, t_2) \left(\hat{\mathcal{O}}_2 \hat{\rho}_{SA}(t_2) \right) \right] \quad (\text{B9})$$

This relation expresses two-time correlation function defined from unitary evolution of the *aux* model in terms of Lindblad-type evolution of $S + A$ subspace of the *aux* model. Finally, we note that while we had restriction $t > 0$ in derivation of (B3), the result is correct also for $t = 0$, as one can see by direct comparison of the two sides in (B9). Eq. (B9) together with (20) leads to (25).

Similarly, for $t_2 \geq t_1 \geq 0$ one can prove that

$$\begin{aligned} \langle \hat{\mathcal{O}}_1(t_1) \hat{\mathcal{O}}_2(t_2) \rangle &= \quad (\text{B10}) \\ \langle \langle I | \mathcal{O}_2^- \mathcal{U}_{SA}(t_1, t_2) \mathcal{O}_1^+ \mathcal{U}_{SA}(t_2, 0) | \rho_{SA}(0) \rangle \rangle \end{aligned}$$

Appendix C: Derivation of Eq. (30)

Here we prove that multi-time correlation functions of arbitrary operators $\hat{\mathcal{O}}_i$ in $S + A$ of the *aux* model defined on the Keldysh contour,

$$\left\langle T_c \hat{\mathcal{O}}_1(\tau_1) \hat{\mathcal{O}}_2(\tau_2) \dots \hat{\mathcal{O}}_N(\tau_N) \right\rangle, \quad (\text{C1})$$

can be evaluated from Markov Lindblad-type evolution in the $S + A$ subspace. Here operators $\hat{\mathcal{O}}_i$ are in the Heisenberg picture. Projections (one-the-contour time orderings) of multi-time correlation functions (C1) will have the following form

$$\begin{aligned} &\left\langle \hat{B}_1(s_1) \hat{B}_2(s_2) \dots \hat{B}_m(s_m) \hat{C}_n(t_n) \dots \hat{C}_2(t_2) \hat{C}_1(t_1) \right\rangle \\ &= \text{Tr} \left[\hat{C}_n(t_n) \dots \hat{C}_2(t_2) \hat{C}_1(t_1) \hat{\rho}^{aux}(0) \right. \\ &\quad \left. \times \hat{B}_1(s_1) \hat{B}_2(s_2) \dots \hat{B}_m(s_m) \right] \quad (\text{C2}) \end{aligned}$$

where $\hat{B}_j(s_j)$ and $\hat{C}_i(t_i)$ are used for operators $\hat{\mathcal{O}}_i$ on the backward and forward branches of the contour, respectively (see Fig. 2) and where

$$\begin{aligned} t_n &> t_{n-1} > \dots > t_1 \geq 0 \\ s_m &> s_{m-1} > \dots > s_1 \geq 0 \end{aligned} \quad (\text{C3})$$

Note, there is no ordering between the sets $\{t_i\}$ and $\{s_j\}$ ($i \in \{1, 2, \dots, n\}$ and $j \in \{1, 2, \dots, m\}$).

Let denote the time-ordering of the set $\{t_1, t_2, \dots, t_n, s_1, s_2, \dots, s_m\}$ by $\{\theta_1, \dots, \theta_{m+n}\}$. So that

$$\theta_{m+n} \geq \theta_{m+n-1} \geq \dots \geq \theta_1 \geq 0. \quad (\text{C4})$$

We want to prove that projections of multi-time correlation functions satisfy quantum regression theorem²⁹

$$\begin{aligned} \langle \langle I | \mathcal{O}_{\theta_{m+n}} \mathcal{U}_{SA}(\theta_{m+n}, \theta_{m+n-1}) \mathcal{O}_{\theta_{m+n-1}} \mathcal{U}_{SA}(\theta_{m+n-1}, \theta_{m+n-2}) \dots \mathcal{O}_{\theta_1} \mathcal{U}_{SA}(\theta_1, 0) | \rho_{SA}(0) \rangle \rangle \end{aligned} \quad (\text{C5})$$

where \mathcal{O}_{θ_i} is superoperator, Eq. (26), corresponding to operator \hat{B} or \hat{C} (backward or forward branch of the contour, respectively) at real time θ_i .

We prove (C5) by mathematical induction. First, we note that Eqs. (25) and (B10) are special cases of Eq. (C5) with $m+n=2$. Suppose that for any combination (m, n) satisfying $m+n=k$, Eq. (C5) holds. Now let consider $(k+1)$ -time correlation function

$$\begin{aligned} &\left\langle \hat{B}_1(s_1) \hat{B}_2(s_2) \dots \hat{B}_m(s_m) \hat{\mathcal{O}}_{\theta_{k+1}}(\theta_{k+1}) \hat{C}_n(t_n) \dots \right. \\ &\quad \left. \dots \hat{C}_2(t_2) \hat{C}_1(t_1) \right\rangle \quad (\text{C6}) \end{aligned}$$

where $\theta_{k+1} > t_n > t_{n-1} > \dots > t_1 \geq 0$ and $\theta_{k+1} > s_m > s_{m-1} > \dots > s_1 \geq 0$. As previously, we time-order both sets,

$$\theta_{k+1} > \theta_k \geq \theta_{k-1} \geq \dots \geq \theta_1 \geq 0, \quad (\text{C7})$$

and take the derivative with respect to the latest time

$$\begin{aligned} &\frac{d}{d\theta_{k+1}} \left\langle \hat{B}_1(s_1) \hat{B}_2(s_2) \dots \hat{B}_m(s_m) \hat{\mathcal{O}}_{\theta_{k+1}}(\theta_{k+1}) \hat{C}_n(t_n) \dots \hat{C}_2(t_2) \hat{C}_1(t_1) \right\rangle \\ &\equiv \frac{d}{d\theta_{k+1}} \langle \langle I | \mathcal{O}_{\theta_{k+1}} \mathcal{U}^{aux}(\theta_{k+1}, \theta_k) \mathcal{O}_{\theta_k} \mathcal{U}^{aux}(\theta_k, \theta_{k-1}) \dots \mathcal{U}^{aux}(\theta_1, 0) | \rho^{aux}(0) \rangle \rangle \\ &= \text{Tr}_{SA} \left\{ \hat{\mathcal{O}}_{\theta_{k+1}} \frac{d}{d\theta_{k+1}} \langle \langle I_{LR} | \mathcal{U}^{aux}(\theta_{k+1}, \theta_k) \mathcal{O}_{\theta_k} \mathcal{U}^{aux}(\theta_k, \theta_{k-1}) \dots \mathcal{U}^{aux}(\theta_1, 0) | \rho^{aux}(0) \rangle \rangle_{LR} \right\} \\ &= \text{Tr}_{SA} \left\{ \hat{\mathcal{O}}_{\theta_{k+1}} \mathcal{L}_{SA}(\theta_{k+1}) \langle \langle I_{LR} | \mathcal{U}^{aux}(\theta_{k+1}, \theta_k) \mathcal{O}_{\theta_k} \mathcal{U}^{aux}(\theta_k, \theta_{k-1}) \dots \mathcal{U}^{aux}(\theta_1, 0) | \rho^{aux}(0) \rangle \rangle_{LR} \right\} \end{aligned} \quad (\text{C8})$$

where we followed the argument leading to (B5) and (B6) in B. In (C8) \mathcal{U}^{aux} is the Liouville space analog of the

Hilbert space evolution operator \hat{U}^{aux} defined in Eq. (24).

Taking into account that \hat{O}_{θ_1} is an arbitrary operator, we get

$$\frac{d}{d\theta_{k+1}} \langle\langle I_{LR} | \mathcal{U}^{aux}(\theta_{k+1}, 0) \dots | \rho^{aux}(0) \rangle\rangle_{LR} = \mathcal{L}_{SA}(\theta_{k+1}) \langle\langle I_{LR} | \mathcal{U}^{aux}(\theta_{k+1}, 0) \dots | \rho^{aux}(0) \rangle\rangle_{LR} \quad (C9)$$

where $\langle\langle I_{LR} | \mathcal{U}^{aux}(\theta_{k+1}, 0) \dots | \rho^{aux}(0) \rangle\rangle_{LR}$ is shorthand notation for the expression introduced in (C8).

Solving (C9) and utilizing quantum regression theorem for its initial condition, $\theta_{k+1} = \theta_k$, leads to

$$\begin{aligned} & \left\langle \hat{B}_1(s_1) \hat{B}_2(s_2) \dots \hat{B}_m(s_m) \hat{O}_{\theta_{k+1}}(\theta_{k+1}) \hat{C}_n(t_n) \dots \hat{C}_2(t_2) \hat{C}_1(t_1) \right\rangle \\ & = \langle\langle I | \mathcal{O}_{\theta_{k+1}} \mathcal{U}_{SA}(t_{\theta_{k+1}}, t_{\theta_k}) \mathcal{O}_{\theta_k} \mathcal{U}_{SA}(t_{\theta_k}, t_{\theta_{k-1}}) \dots \mathcal{O}_{\theta_1} \mathcal{U}_{SA}(t_{\theta_1}, 0) | \rho_{SA}(0) \rangle\rangle \end{aligned} \quad (C10)$$

which is quantum regression theorem for $(k+1)$ -time correlation function.

Thus, by induction we prove Eq. (30).

-
- * Electronic address: migalperin@ucsd.edu
- ¹ L. Jiang, J. S. Hodges, J. R. Maze, P. Maurer, J. M. Taylor, D. G. Cory, P. R. Hemmer, R. L. Walsworth, A. Yacoby, A. S. Zibrov, et al., *Science* **326**, 267 (2009), ISSN 0036-8075, 1095-9203, URL <https://science.sciencemag.org/content/326/5950/267>.
 - ² S. Khasminkaya, F. Pyatkov, K. Sowik, S. Ferrari, O. Kahl, V. Kovalyuk, P. Rath, A. Vetter, F. Hennrich, M. M. Kappes, et al., *Nat. Photon.* **10**, 727 (2016), ISSN 1749-4885, 1749-4893, URL <http://www.nature.com/articles/nphoton.2016.178>.
 - ³ A. Gaita-Ariño, F. Luis, S. Hill, and E. Coronado, *Nature Chem.* **11**, 301 (2019), ISSN 1755-4330, 1755-4349, URL <http://www.nature.com/articles/s41557-019-0232-y>.
 - ⁴ F. B. Anders, *Phys. Rev. Lett.* **101**, 066804 (2008), URL <http://link.aps.org/abstract/PRL/v101/e066804>.
 - ⁵ S. Schmitt and F. B. Anders, *Phys. Rev. B* **81**, 165106 (2010).
 - ⁶ F. Wegner, *Annalen der Physik* **506**, 77 (1994).
 - ⁷ S. Kehrein, *The Flow Equation Approach to Many-Particle Systems*, vol. 217 of *Springer Tracts in Modern Physics* (Springer-Verlag, 2006).
 - ⁸ U. Schollwöck, *Rev. Mod. Phys.* **77**, 259 (2005).
 - ⁹ U. Schollwöck, *Ann. Phys.* **326**, 96 (2011).
 - ¹⁰ H. Wang and M. Thoss, *J. Chem. Phys.* **131**, 024114 (2009).
 - ¹¹ H. Wang and M. Thoss, *Chem. Phys.* **509**, 13 (2018).
 - ¹² G. Cohen, E. Gull, D. R. Reichman, and A. J. Millis, *Phys. Rev. Lett.* **115**, 266802 (2015).
 - ¹³ A. E. Antipov, Q. Dong, J. Kleinhenz, G. Cohen, and E. Gull, *Phys. Rev. B* **95**, 085144 (2017).
 - ¹⁴ M. Ridley, V. N. Singh, E. Gull, and G. Cohen, *Phys. Rev. B* **97**, 115109 (2018).
 - ¹⁵ V. Anisimov and Y. Izyumov, *Electronic Structure of Strongly Correlated Materials* (Springer, 2010).
 - ¹⁶ H. Aoki, N. Tsuji, M. Eckstein, M. Kollar, T. Oka, and P. Werner, *Rev. Mod. Phys.* **86**, 779 (2014).
 - ¹⁷ E. Arrigoni, M. Knap, and W. von der Linden, *Phys. Rev. Lett.* **110**, 086403 (2013).
 - ¹⁸ A. Dorda, M. Nuss, W. von der Linden, and E. Arrigoni, *Phys. Rev. B* **89**, 165105 (2014).
 - ¹⁹ F. Chen, G. Cohen, and M. Galperin, *Phys. Rev. Lett.* **122**, 186803 (2019), ISSN 0031-9007, 1079-7114, URL <https://link.aps.org/doi/10.1103/PhysRevLett.122.186803>.
 - ²⁰ F. Schwarz, M. Goldstein, A. Dorda, E. Arrigoni, A. Weichselbaum, and J. von Delft, *Phys. Rev. B* **94** (2016), ISSN 2469-9950, 2469-9969, URL <https://link.aps.org/doi/10.1103/PhysRevB.94.155142>.
 - ²¹ A. Dorda, M. Sorantin, W. v. d. Linden, and E. Arrigoni, *New J. Phys.* **19**, 063005 (2017), ISSN 1367-2630, URL <http://stacks.iop.org/1367-2630/19/i=6/a=063005?key=crossref.42dc685e6598dd769ff438461d08de1c>.
 - ²² E. Arrigoni and A. Dorda, *Master Equations Versus Keldysh Green's Functions for Correlated Quantum Systems Out of Equilibrium* (Springer International Publishing, Cham, 2018), pp. 121–188, ISBN 978-3-319-94956-7, URL https://doi.org/10.1007/978-3-319-94956-7_4.
 - ²³ D. Tamascelli, A. Smirne, S. Huelga, and M. Plenio, *Phys. Rev. Lett.* **120** (2018), ISSN 0031-9007, 1079-7114, URL <https://link.aps.org/doi/10.1103/PhysRevLett.120.030402>.
 - ²⁴ A. Imamoglu, *Phys. Rev. A* **50**, 3650 (1994), ISSN 1050-2947, 1094-1622, URL <https://link.aps.org/doi/10.1103/PhysRevA.50.3650>.
 - ²⁵ A. Dorda, M. Ganahl, H. G. Evertz, W. von der Linden, and E. Arrigoni, *Phys. Rev. B* **92**, 125145 (2015), ISSN 1098-0121, 1550-235X, URL <https://link.aps.org/doi/10.1103/PhysRevB.92.125145>.
 - ²⁶ C. Jung, A. Lieder, S. Brener, H. Hafermann, B. Baxevanis, A. Chudnovskiy, A. Rubtsov, M. Katsnelson, and A. Lichtenstein, *Ann. Phys. (Berlin)* **524**, 49 (2012), ISSN 1521-3889, URL <http://dx.doi.org/10.1002/andp.201100045>.
 - ²⁷ B. Bauer, L. D. Carr, H. G. Evertz, A. Feiguin, J. Freire, S. Fuchs, L. Gamper, J. Gukelberger, E. Gull, S. Guertler, et al., *J. Stat. Mech.* p. 35 (2011).
 - ²⁸ M. Dolfi, B. Bauer, S. Keller, A. Kosenkov, T. Ewart, A. Kantian, T. Giamarchi, and M. Troyer, *Computer Physics Communications* **185**, 3430 (2014).
 - ²⁹ H.-P. Breuer and F. Petruccione, *The Theory of Open Quantum Systems* (Oxford University Press, 2003).